

UCLA

UCLA Previously Published Works

Title

Little Ice Age climatic erraticism as an analogue for future enhanced hydroclimatic variability across the American Southwest.

Permalink

<https://escholarship.org/uc/item/6m31k390>

Journal

PloS one, 12(10)

ISSN

1932-6203

Authors

Loisel, Julie
MacDonald, Glen M
Thomson, Marcus J

Publication Date

2017

DOI

10.1371/journal.pone.0186282

Peer reviewed

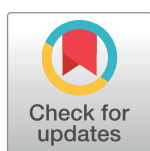
RESEARCH ARTICLE

Little Ice Age climatic erraticism as an analogue for future enhanced hydroclimatic variability across the American Southwest

Julie Loisel^{1,2,3*}, Glen M. MacDonald^{2,3}, Marcus J. Thomson³

1 Department of Geography, Texas A&M University, Eller O&M Building, College Station TX, **2** Institute of the Environment and Sustainability, University of California Los Angeles, La Kretz Hall, Los Angeles CA, **3** Department of Geography, University of California Los Angeles, Bunche Hall, Los Angeles CA

* juloisel@hotmail.com



Abstract

The American Southwest has experienced a series of severe droughts interspersed with strong wet episodes over the past decades, prompting questions about future climate patterns and potential intensification of weather disruptions under warming conditions. Here we show that interannual hydroclimatic variability in this region has displayed a significant level of non-stationarity over the past millennium. Our tree ring-based analysis of past drought indicates that the Little Ice Age (LIA) experienced high interannual hydroclimatic variability, similar to projections for the 21st century. This is contrary to the Medieval Climate Anomaly (MCA), which had reduced variability and therefore may be misleading as an analog for 21st century warming, notwithstanding its warm (and arid) conditions. Given past non-stationarity, and particularly erratic LIA, a 'warm LIA' climate scenario for the coming century that combines high precipitation variability (similar to LIA conditions) with warm and dry conditions (similar to MCA conditions) represents a plausible situation that is supported by recent climate simulations. Our comparison of tree ring-based drought analysis and records from the tropical Pacific Ocean suggests that changing variability in El Niño Southern Oscillation (ENSO) explains much of the contrasting variances between the MCA and LIA conditions across the American Southwest. Greater ENSO variability for the 21st century could be induced by a decrease in meridional sea surface temperature gradient caused by increased greenhouse gas concentration, as shown by several recent climate modeling experiments. Overall, these results coupled with the paleo-record suggests that using the erratic LIA conditions as benchmarks for past hydroclimatic variability can be useful for developing future water-resource management and drought and flood hazard mitigation strategies in the Southwest.

OPEN ACCESS

Citation: Loisel J, MacDonald GM, Thomson MJ (2017) Little Ice Age climatic erraticism as an analogue for future enhanced hydroclimatic variability across the American Southwest. PLoS ONE 12(10): e0186282. <https://doi.org/10.1371/journal.pone.0186282>

Editor: Xiaoyan Yang, Chinese Academy of Sciences, CHINA

Received: June 18, 2017

Accepted: September 28, 2017

Published: October 16, 2017

Copyright: © 2017 Loisel et al. This is an open access article distributed under the terms of the [Creative Commons Attribution License](https://creativecommons.org/licenses/by/4.0/), which permits unrestricted use, distribution, and reproduction in any medium, provided the original author and source are credited.

Data Availability Statement: PDSI values from the North American Drought Atlas (version 2a) are available online at <http://www.ncdc.noaa.gov/paleo/pdsi.html>. The dataset can also be downloaded here: <https://iridl.ldeo.columbia.edu/SOURCES/LDEO/TRL/NADAv2a-2008/PDSI/datafiles.html>.

Funding: This research was supported by the Department of Interior Southwest Climate Science Center core grant to UCLA (GMM). The funders had no role in study design, data collection and

Introduction

Over the past century, water management has relied on the principle of stationarity, which assumes that historical hydroclimatic variations provide an envelope within which future conditions are expected. However, some areas of the American Southwest will likely become periodically more arid than the range of observations recorded over the last century [1,2], and thus

analysis, decision to publish, or preparation of the manuscript.

Competing interests: The authors have declared that no competing interests exist.

the assumption of stationarity for forecasting future hydroclimatic variability is not justified [3]. Several studies suggest that, along with warmer mean temperatures, climate variability is likely to increase [4,5]. As climate variability increases, the frequency of extreme events is likely to increase as well [4], with direct consequences in the Southwest. For example, an increase in the frequency or magnitude of floods and droughts could lead to yield reductions, crop damage, and crop failure [6]. Warmer and more variable conditions would also impact ecological systems, with one of the most important aspects being fire regimes [7,8] and populations of vulnerable species [9]. Enhanced variability in precipitation promotes fire in many wildland systems [10–13]. Therefore, identifying strategies for water-resource management under changing climate variability, and not just changes in the mean state, is necessary [14].

Instrumental records have shown that hydroclimatic variability across the American Southwest is mostly structured around cool-season precipitation regimes, with a few winter storms typically contributing a disproportionately large amount of the annual precipitation across this region [15]. That is particularly the case in California, where decadal precipitation variance is typically equivalent to 20–50% of mean annual averages, mostly because of changes in precipitation received between November and March [16–17]. As a result, small surpluses or deficits in the number of precipitation events translate into relatively large hydroclimatic swings from wet to dry years. In addition to providing a considerable fraction of the annual total amount, winter precipitation tends to remain in the 'terrestrial' hydrological cycle (i.e., part of stream flow) much longer than the summer fraction [17], making the cool-season precipitation regime particularly important for natural processes and human consumption. The large inter-annual to decadal hydroclimatic variability in winter precipitation is highly influenced by sea surface temperature (SST) anomalies in the tropical Pacific Ocean and associated changes in large-scale atmospheric circulation patterns [16]. In general, cool SSTs in the eastern tropical Pacific (La Niña conditions) tend to induce arid conditions in the Southwest, whereas warmer SSTs (El Niño conditions) are associated with relatively wet conditions [18,19].

Temporal precipitation variability in the Southwest may increase significantly at the decadal and multi-decadal scale over the 21st century. Several climate predictions for future impacts of increasing radiative forcing suggest warming in the eastern Pacific and a more variable ENSO system, with ~70% chance of stronger and/or more frequent El Niño conditions, and a ~50% chance of increased frequency in La Niñas (Fig 1; [20,21]). Such potential changes in variability are in agreement with instrumental records and paleoclimate reconstructions, which show that the magnitude and trend of hydroclimatic variability has not been constant in the Southwest during the Common Era (C.E.). As such, recent studies looking back at the past 30 years of data show a decadal modulation of El Niño Southern Oscillation (ENSO) stability, with the past decade characterized by higher-frequency and lower-amplitude El Niños than the previous ones [22]. In addition, the unified ENSO proxy (UEP) time series, which combines information from 10 globally distributed ENSO reconstructions, displays a rising trend toward enhanced ENSO variance since 1650 CE (Fig 2; [23]).

On land, multimodel mean PDSI time-series projections for the coming century indicate that drought risk could reach an all-time high during the late 21st century, with unprecedented drought conditions that might exceed those of the MCA [2,24]. These modeled PDSI values are also characterized by high variance [Fig 2], reinforcing the hypothesis that the coming century will likely be faced with high hydroclimatic variability that could be linked to ENSO dynamics. These results remain speculative however, as there are large differences in PDSI projections between models [Fig 2].

The Medieval Climate Anomaly (MCA, ~950–1400 CE) is often used as an analog for 21st century hydroclimate because it represents a warm (and arid) period. The MCA appears related to general surface warming in the Northern Hemisphere, prolonged La Niña

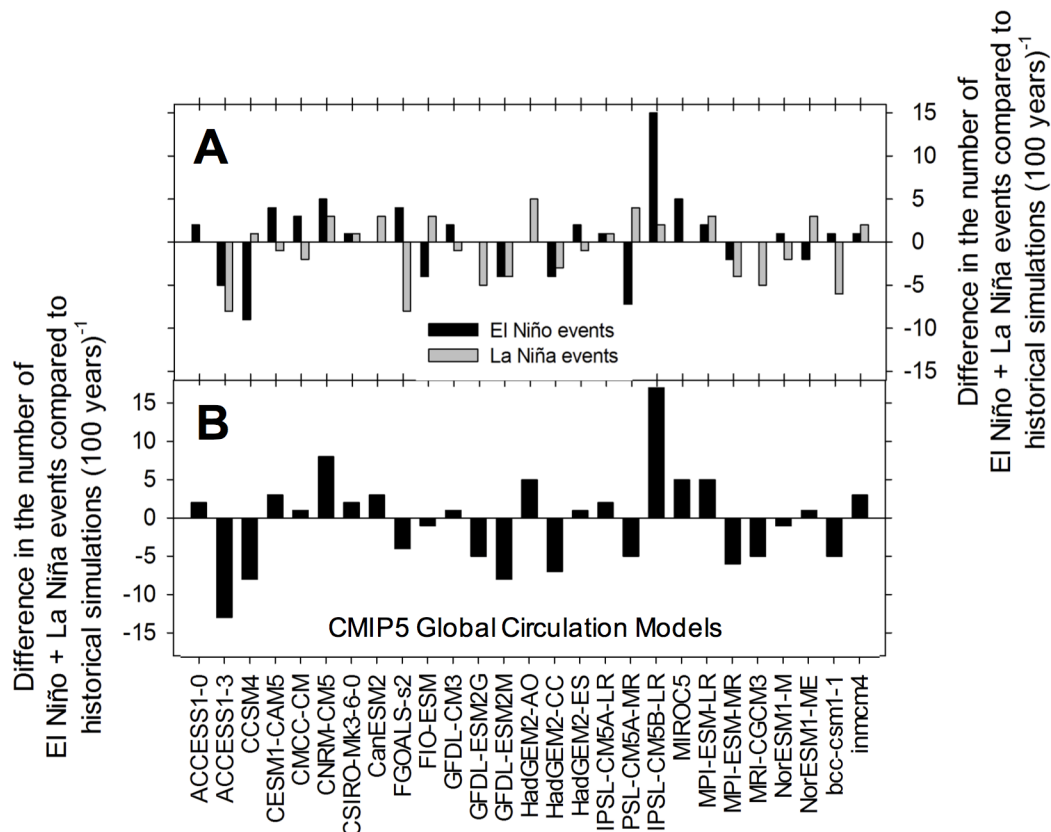


Fig 1. Predicted number of El Niño and La Niña events during the 21st century compared to historical simulations. Data are based on 27 CMIP5 models and using the RCP8.5 scenario. The overall sum of predicted El Niño events is +10, while that of La Niñas is -19. Overall, 70% of the models indicate either no change or an increase in the number of El Niño events for the coming century; this figure goes down to 52% for La Niñas (data from 21).

<https://doi.org/10.1371/journal.pone.0186282.g001>

conditions [18, 25–28], and a persistent positive North Atlantic Oscillation mode [29]. It has been referred to as a stable time interval with ‘quiet’ conditions in regards to low perturbation by external radiative forcing [30]. In this study, we demonstrate that the Little Ice Age (LIA, ~1400–1850 CE) might be more representative of future hydroclimatic variability than the conditions during the MCA megadroughts for the American Southwest, and thus provide a useful scenario for development of future water-resource management and drought and flood hazard mitigation strategies.

Materials and methods

Paleohydrological reconstructions and model simulations

Tree ring-derived Palmer Drought Severity Index (PDSI) time series have been widely used to estimate the spatial extent, duration, timing, and intensity of droughts from the past millennium across the American Southwest [31–37], but the amplitude and variance of hydroclimatic variability have received significantly less attention (but see [38]). We used PDSI values from the North American Drought Atlas (NADA, version 2a) to detect changes in aridity variability and periodicity for the Southwest over the past millennium. The NADA consists of a network of 286 gridded data points (2.5° x 2.5°) covering North America that is based on annually resolved tree ring chronologies [39,40]. Information related to reconstruction

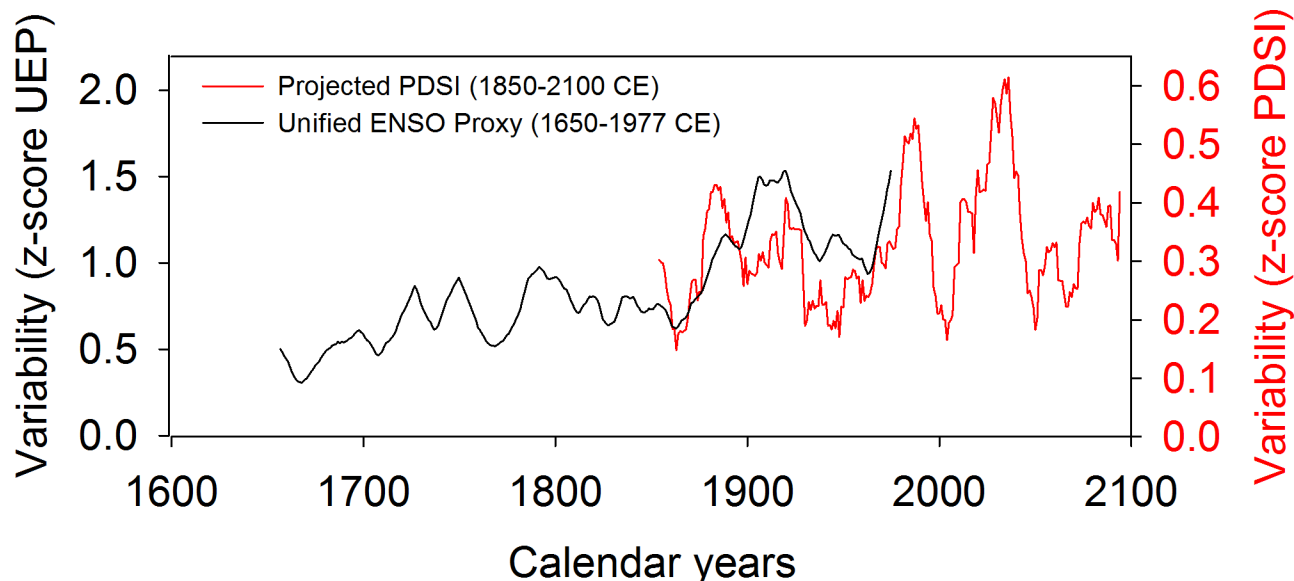


Fig 2. Unified ENSO proxy (UEP) variability compared to projected PDSI variability across the American Southwest in the coming century. The UEP (in black) combines ENSO and PDO/IPO Pacific climate variability and is based on 10 commonly used ENSO proxies that were consolidated via Principal Component Analysis to capture the joint features of these reconstructions (data from 23). The multimodel mean summer (JJA) PDSI variability over the American Southwest for 1850–2100 (in red) is based on 17 CMIP5 model projections and using the RCP 8.5 emissions scenario (data from 24).

<https://doi.org/10.1371/journal.pone.0186282.g002>

methods can be found in [39]. Grid points that cover the western Southwest (32.5–37.5°N, 115–122.5°W, $n = 9$ grid cells) were selected on the basis of their climatology [Fig 3]. Annual PDSI values for these study regions were obtained from 950 to 2006 CE.

The El Junco diatom index record from the Galápagos Islands (0°54'S, 89°29'W, 43) and the fossil-coral oxygen isotopic records from Palmyra Island (6°N, 162°W, 44) constitute ENSO-sensitive proxy records from the equatorial Pacific against which we compared our results. Both records were resampled at an annual time step prior to statistical analysis. Information related to the study sites, reconstruction methods, and chronologies can be found in the original publications [41,42].

Winter precipitation data for the past millennium were obtained from the Community Earth System Model's Last Millennium Ensemble Project (CESM LME) [43]. CESM LME generated ten ensemble members with 'full' forcing, which consists of transient solar output, volcanic activity, land use, greenhouse gases, and orbital dynamics for the complete 850–2005 time series, as well as ozone-aerosol forcing for the 1850–2005 series used for bias correction. The ensemble member approach is commonly used to approximate a measure of uncertainty in modeled results. We analyzed months November through February to represent ENSO influence on the regional precipitation regime. We used ensemble members 2 to 5, which consist of coupled ocean-atmosphere climate models; outputs represent a range of probable monthly precipitation values generated by CESM. Precipitation data were bias corrected using NOAA's CPC US unified daily precipitation data provided by NOAA/OAR/ESRL PSD [<http://www.esrl.noaa.gov/psd/>]. Grid cells over the Pacific were excluded from the analysis.

Statistical analyses

Variability measures applied to NADA PDSI, El Junco diatoms, Palmyra isotopes, and modeled precipitation from CESM were developed from the original, raw time series. Each time



Fig 3. Study region. North American Drought Atlas (NADA) gridded dataset (<http://www.ncdc.noaa.gov/paleo/pdsi.html>; <https://iridl.ldeo.columbia.edu/SOURCES/.LDEO/.TRL/.NADAv2a-2008/PDSI/datafiles.html>) used in this study. The bold black line delineates the western portion of the American Southwest.

<https://doi.org/10.1371/journal.pone.0186282.g003>

series was filtered (10-year high-pass) using AnalySeries 2.0.4.2 [44] to preserve variability in the ENSO band at 2 to 8 years [45]. Variance was then computed as the 10-year running standard deviation of each filtered time series [38] and rescaled to z-scores.

Student's t-tests were used to determine whether or not the MCA (950–1400 CE), LIA (1400–1850 CE), and RW (1850–2006) datasets were significantly different from each other in terms of their variance. Lastly, a bias-corrected wavelet analysis was used to identify dominant

periodicities in the unfiltered mean PDSI time series between the MCA, LIA, and RW [46]. Tolerance level for significance of dominant frequencies against red-noise background spectrum was set at 0.95 [47].

Results

Paleohydrological reconstructions

Analyses performed on the NADA PDSI time series show a number of important and statistically significant differences in hydroclimatic variability between the MCA, LIA, and RW (Table 1, Fig 4). Variance in PDSI amplitude is significantly lower during the MCA than during the LIA and the RW (Tukey's LSD: $p < 0.001$). Likewise, mean running variance is overall lower ($p < 0.001$) during the MCA than during the LIA and the RW (Fig 4C). The evolution of change in drought amplitude from the MCA to the LIA continues during the RW, with LIA variance being indistinguishable from that recorded during the RW ($p = 0.22$). In addition, the evolution of change in drought amplitude clearly shows greatest variance during the LIA, with

Table 1. Moments of the distribution of filtered paleoecological records and climate simulations.

| dataset | time period | mean of running variance | standard dev. of running variance |
|---|-------------|--------------------------|-----------------------------------|
| Western Southwest PDSI (CA-NV) | MCA | 1.66*** | 0.49 |
| | LIA | 1.91*** | 0.47 |
| | RW | 1.86*** ¹ | 0.46 |
| El Junco | MCA | 0.08*** | 0.03 |
| | LIA | 0.12*** | 0.05 |
| | RW | 0.18*** ² | 0.05 |
| Palmyra | MCA | 0.09** | 0.02 |
| | LIA | 0.10** | 0.03 |
| | RW | 0.12** | 0.02 |
| Winter P (NDJF), CESM em002 | MCA | 0.04 | 1.17 |
| | LIA | -0.04 | 0.89 |
| | RW | -0.10 | 0.73 |
| Winter P (NDJF), CESM em003 | MCA | 0.13*** | 1.67 |
| | LIA | -0.12*** | 0.91 |
| | RW | -0.02 | 1.01 |
| Winter P (NDJF), CESM em004 | MCA | -0.02 | 0.99 |
| | LIA | 0.01 | 1.02 |
| | RW | 0.02 | 0.95 |
| Winter P (NDJF), CESM em005 | MCA | 0.13** | 0.99 |
| | LIA | -0.05** | 1.02 |
| | RW | -0.24** | 0.91 |
| Winter P (NDJF), CESM averaged em002 to em005 | MCA | -0.13 | 0.99 |
| | LIA | -0.17 | 1.02 |
| | RW | 0.89*** ³ | 0.91 |

*Statistical significance at $p < 0.1$.

**Statistical significance at $p < 0.05$.

***Statistical significance at $p < 0.01$.

¹The RW is statistically different from the MCA ($p < 0.01$), but indistinguishable from the LIA ($p = 0.22$).

²The RW time series from El Junco was not used in the statistical analysis as it only contains 5 data points.

³The RW is statistically different from the MCA and the LIA ($p < 0.05$).

<https://doi.org/10.1371/journal.pone.0186282.t001>

roughly half (53%) of years for which PDSI's mean running variance stays within the highest 10th percentile (Fig 4B).

A wavelet analysis reveals changes in relative domains of variability over time, with a higher concentration of power in the interannual and decadal bands during the LIA that is much subdued during the MCA (Fig 4D). This shift in quasi-periodic variance confirms the presence of a change in the dominant frequencies of variability between the MCA and LIA boundary. An increase in power of the higher frequency ENSO band of 3 to 8 years was detected, especially after 1550 CE. These shifts in PDSI periodicity combined with a general increase in variance are concomitant with the transition from the MCA to the LIA.

Evidence of similar changes in variance and variability are clear from ENSO-sensitive proxy records from the equatorial Pacific (Fig 5, Table 1). The fossil-coral oxygen isotopic

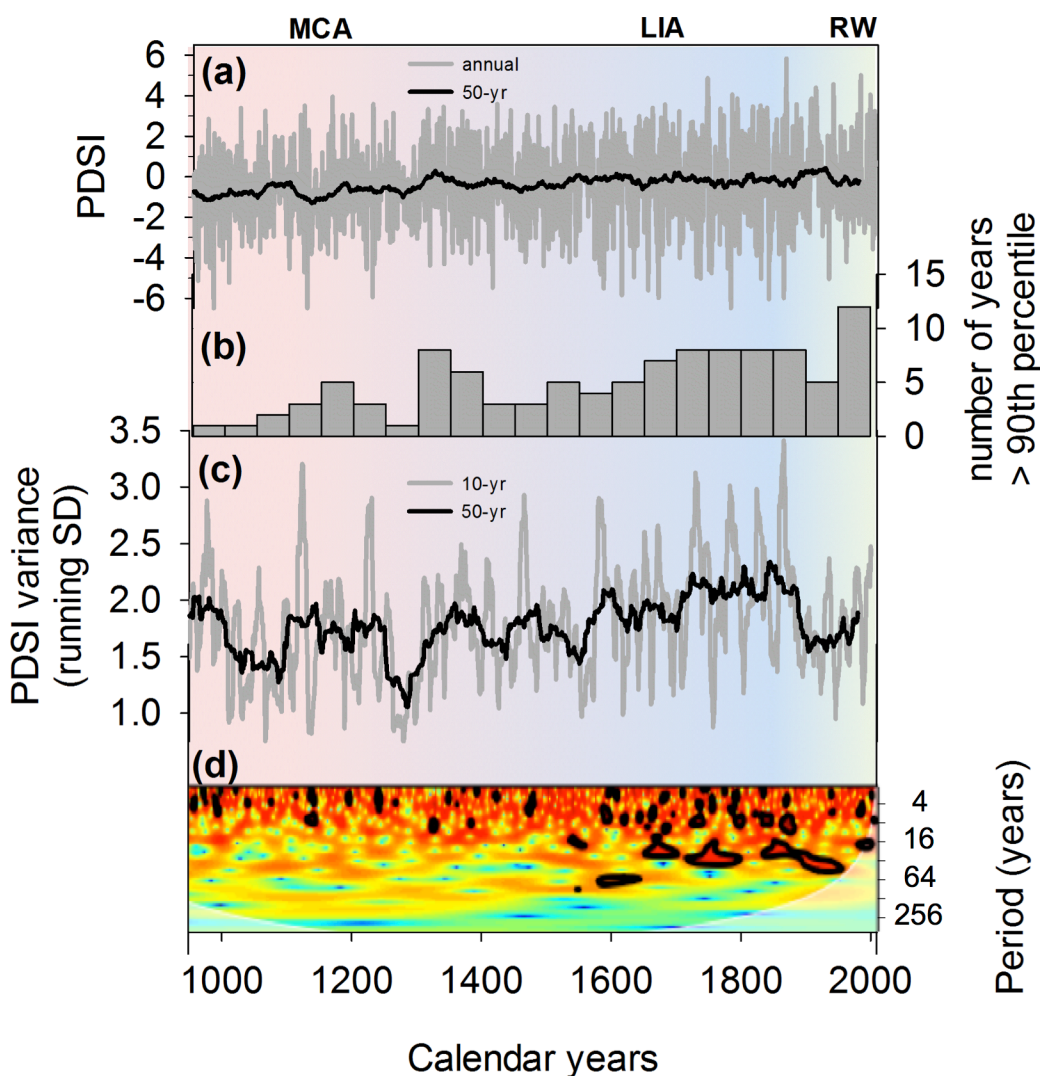


Fig 4. Palmer Drought Severity Index (PDSI) variability in the American Southwest over the past millennia. The annual time series (a) displays greater variability during the LIA than the MCA, as indicated by the number of years during which variability is above the 90th percentile (b). The time series was filtered using a 10-year high-pass to compute a time series of PDSI variance (c) on the basis of 10-year and 50-year running standard deviations (SD). A wavelet analysis shows the evolution of the power spectrum of tree-ring derived PDSI over the past millennia (d). The black contours are the 10% significance regions, using a red-noise background spectrum [46].

<https://doi.org/10.1371/journal.pone.0186282.g004>

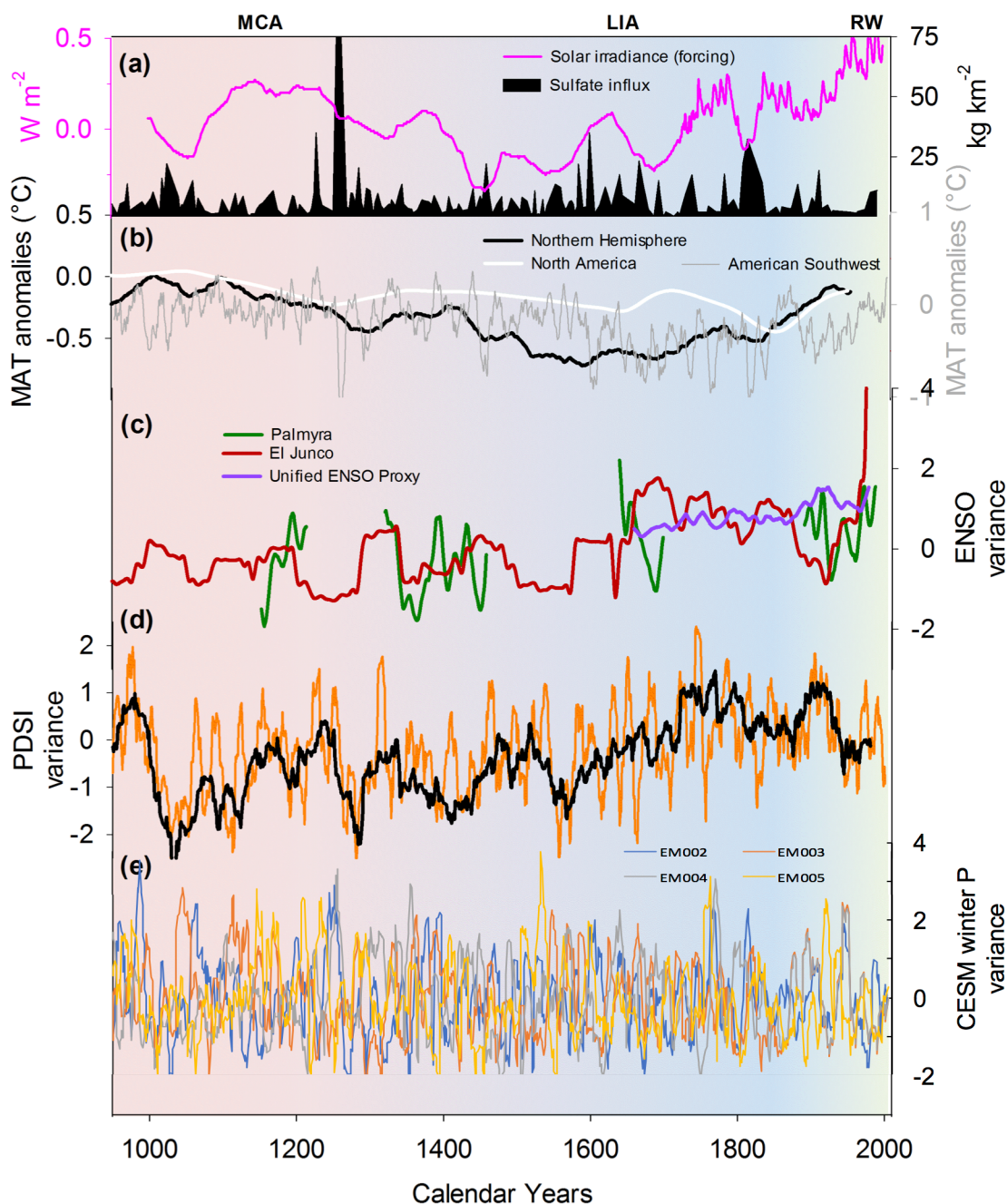


Fig 5. Factors affecting and reflecting hydrologic variability in the American Southwest over the past millennia. Global solar irradiance reconstruction [48–50] and ice-core based sulfate (SO_4) influx in the Northern Hemisphere [51] from volcanic activity (a); mean annual temperature (MAT) reconstructions for the Northern Hemisphere [52], North America [29], and the American Southwest* expressed as anomalies based on 1961–1990 temperature averages (b); changes in ENSO-related variability based on El Junco diatom record [41], oxygen isotopes records from Palmyra [42], and the unified ENSO proxy [UEP; 23] (c); changes in PDSI variability for the American Southwest (d), and changes in winter precipitation variability as simulated by CESM model ensembles 2 to 5 [43]. *Data for the American Southwest temperature reconstruction is from PRISM temperature data from CMIP5 [43].

<https://doi.org/10.1371/journal.pone.0186282.g005>

records ($\delta^{18}\text{O}$) from Palmyra Island present similar, and climatologically consistent, changes to the Southwest PDSI variance over time, including decreased mean state of ENSO in the MCA (a cooler eastern equatorial Pacific) and more intense ENSO in the LIA, particularly

during the mid-seventeenth century. Variance in $\delta^{18}\text{O}$ amplitude was lower during the MCA than during the LIA and the RW (Table 1). Likewise, mean running variance was lower overall ($p < 0.001$) during the MCA than during the LIA and the RW. As the Palmyra fossil-coral records are not continuous, these statistics should be used with caution. That said, the continuous diatom record from El Junco in the Galápagos Islands similarly shows enhanced ENSO variability during the LIA when compared to the past millennium (not shown). Noteworthy is the significantly lower variance ($p = 0.02$) in the diatom index during the MCA when compared to that of the LIA. Likewise, mean running variance was overall lower during the MCA than during the LIA. As there are only five data points characterizing the RW, results were considered inconclusive (Table 1).

Model simulations

Mean modeled winter precipitation from CESM LME ensemble members 2 to 5 show unsystematic differences in Southwest winter precipitation variability between each other and with our NADA PDSI time series (Table 1, S1 Fig). For instance, mean variance of MCA winter precipitation amounts was more variable than those of the LIA for ensemble members 3 and 5 ($p < 0.05$). Likewise, mean variance in winter precipitation during the RW was lower than those simulated for the LIA and MCA in ensemble member 5 ($p < 0.05$). None of the statistical analysis pertaining to interannual variability in ensemble members 2 and 4 returned significant relationships. Averaging across all 4 model ensembles, we find more variable conditions during the RW than the MCA and LIA ($p < 0.001$), but no difference between the MCA and the LIA ($p = 0.46$).

Data interpretation

The evidence presented here shows that the changes observed in PDSI running variance for the Southwest are coeval with changes in ENSO variance observed in other tropical Pacific Ocean records (Fig 5). The linkages between these changes in Southwest hydroclimatic variance and changes in the Pacific are consistent with modeled and observed historical teleconnections between the Pacific and North America [19,25] and, taken together, support a pervasive relationship between the evolution and variability of the ENSO system and the evolution of drought amplitude and variability in the Southwest [38]. These changes in tropical Pacific Ocean SSTs over the past millennium have often been associated with internal variability of the ocean-atmosphere system [19,27,53,54] that may not be accurately represented in current climate models. The latter would explain the lack of coherence in terms of variability between CESM-derived winter precipitation ensemble members and NADA-derived hydroclimatic conditions across the American Southwest. Model error in representing the impact of SST anomalies on land is also possible. Noteworthy is that model variability is reflecting volcanic forcing rather than changes in ENSO variability.

Discussion

Climate forcing factors during the past millennium

Radiative forcing due to changes in solar irradiance and volcanic activity were arguably important drivers in the MCA and LIA [Fig 5]. For example, the minima in solar irradiance combined to the increase in explosive volcanism after the 12th century have been proposed as mechanisms capable of explaining the cooler LIA conditions [55–57]. Likewise, the period of relative stability in terms of solar irradiance combined with minimal volcanic activity could have induced the MCA [30]. These changes in external forcing could partly explain the change

in variance and periodicity found in our analysis of PDSI between the MCA and LIA [Fig 4]. As future changes in total solar irradiance and volcanic activity remain unknown, they are not included in radiative forcing calculations used for future climate simulations [58]. These forcing factors constitute additional elements that could drive variability in the future, particularly volcanic aerosols following large eruptions [59,60]. In addition, internal variability in the global ocean-atmosphere system as well as stochastic atmospheric variability could lead to additional uncertainty regarding future climate variability [54,61,62]. Our study stresses the importance of those internal connections between tropical Pacific Ocean SSTs, the ENSO system, and the American Southwest hydroclimatic conditions and supports the contention that: (1) internal variability of the ocean-atmosphere system may not be accurately represented in current global climate models, and (2) enhanced variability as a result of these stochastic events should be further considered.

The impact of ENSO on precipitation variability across the Southwest

Our understanding of ENSO and its connection to background climatic conditions comes largely from the paleoclimate record and model simulations. We know that ENSO was systematically weaker during the early and middle Holocene, probably as a consequence of boreal summer perihelion and associated change in length and timing of seasons [63]. Orbital forcing combined with a waning Laurentide ice sheet thus suppressed ENSO until around 5000 ka (1 ka = 1000 calibrated years before present), after which its behavior emerged from records of the Pacific region [42]. The drivers of change in the ENSO regime over the past millennium differ from those in the mid-Holocene. The former is the result of internal variability and radiative forcing (solar output and volcanic activity) rather than long-term changes in Earth's orbital geometry. While there is evidence of a persistent relationship between periods of aridity during the mid-Holocene and the MCA, as both are associated with increases in radiation and cooler SST in the eastern Pacific [64], climate simulations suggest that current forcing by increased GHG may produce an opposite oceanic response in the future [65]. Indeed, an increase in GHG could lead to surface warming over the eastern Pacific followed by an expansion of the warm pool. This would result in decreases in both the meridional and the east-west SST gradients. Those conditions could lead to an increase in ENSO amplitude and/or frequency [21,22,65–67]. While we cannot assert with confidence whether this ongoing shift is part of natural ENSO variability or a manifestation of GHG-induced climate change [68], this increase in variance coincides with rising temperatures in the Western Pacific Warm Pool [23,69–71]. As further warming is anticipated in this region of the Pacific and elsewhere, enhanced hydroclimatic variability might be expected across southwestern North America in the coming century. In addition to potential changes in the mean state of the eastern Pacific Ocean, it is therefore important to consider how interannual and decadal-scale variability in the ENSO system, and thus variability in Southwest hydroclimatology, might evolve over the 21st century [68]. We know that ENSO behavior exhibits decadal- to centennial-scale modulation larger than those observed in the instrumental record [72], and that future conditions could, therefore, push the ENSO system beyond the range of return intervals and levels [3].

A 'warm LIA' as a future climate scenario

In the coming century, increasing atmospheric GHG concentration and associated warming could have important hydrological and water resource consequences in the Southwest resulting from mean state changes due to higher evaporation and decreased precipitation [73–75]. This is in addition to the probable role of GHG-induced amplification of the atmospheric waves in the mid- and high-latitudes, which are thought to lead to increased extreme events

across the Southwest and beyond [76,77]. However, changing climatic variability is also a concern. In addition to influencing management of regional water supplies and agricultural practices as well as modulating droughts and floods [4,5,78–79], interannual hydroclimatic variability directly affects wildland plant growth, fuel conditions, and fire regime. As such, increasing variability in moisture conditions have been linked to enhanced fires, as wet/dry oscillations promote rapid biomass growth and natural fire suppression (fuel accumulation), followed by subsequent burning [8,10–13]. Increasing drought frequency and warming temperatures (fuel moisture) have also been positively associated with increased wildfire activity, particularly in Western North America [39,80–84]. In the Southwest, it has previously been shown that largest fire years tend to be experienced after a wet-dry sequence [7], and in association with an El Niño-La Niña sequence. A pattern of enhanced fire activity during times of increased variability in ENSO and Southwest hydroclimatic conditions could imply a trajectory towards a more fire-prone Southwest during the 21st century [7,13]. Projected warming and drying in spring and summer combined with earlier snowmelt and more winter rain would likely exacerbate this trend by facilitating fire ignition and diminishing fuel moisture during the dry season [85].

In light of our findings and its implications, we propose a 'warm LIA' scenario for the Southwest, which compounds the effects of warmer temperatures with higher hydroclimate variability. Under this previously non-analogue scenario, enhanced drought-prone conditions would be interspersed with flood-prone ones against a background of overall water resource diminishment. Warmer temperatures would alter the rain/snow ratio during the cold season, further increasing the chance for more extreme winter floods and summer droughts [15]. In agreement with this speculation are climate projections suggesting increased flood magnitude in the future across the Southwest, despite reduced mean precipitation amounts [4].

Conclusion

Forecasting hydroclimatic conditions in the American Southwest requires thorough consideration of regional climate non-stationarity in the higher moments and not just mean state. This region is inherently prone to highly variable precipitation, including episodic droughts as well as rapid snowmelt and severe rainstorms that often lead to flooding. Our results show that hydroclimatic variability in the Southwest has not remained constant over the last millennia, with a shift from low to high variance at the MCA-LIA transition that was accompanied by a change in quasi-periodic variance, from a higher concentration of power in the multi-decadal periodicities during the MCA vs. interannual and decadal periodicities during the LIA. Shifts in variance are corroborated by ENSO-sensitive proxy records from the tropical Pacific, suggesting an interactive relationship between the ENSO system and the evolution of drought amplitude in the Southwest. In line with a potential increase in decadal variability in the ENSO system over the 21st century [86], we argue that LIA variability provides crucial targets in the paleoclimate record against which to scale the importance of future hydroclimatic variability in the American Southwest. This finding does not preclude the importance of Medieval-era droughts as benchmarks to assess the severity of future drought risks [24,25,37]. Rather, we propose the possible development of a 'warm LIA' climate scenario for the coming century that combines high precipitation variability (similar to LIA conditions) with warm and dry conditions. These observations further challenge assumptions of climate stationarity and offer new awareness of climate risks for ensuring sustainable water and land management in the Southwest. These observations can also be useful in efforts to understand and reduce model uncertainties related to ENSO behavior and impacts in attempts to model future Southwest climate.

Supporting information

S1 Fig. Winter precipitation variance in the American Southwest for the past millennium, as simulated by CESM LME. We used ensemble members 2 to 5, which consist of coupled ocean-atmosphere climate models; outputs represent a range of probable monthly precipitation values generated by CESM [43].

(PDF)

Acknowledgments

This research was supported by the Department of Interior Southwest Climate Science Center core grant to UCLA (G11AC90008 to GMM).

Author Contributions

Conceptualization: Julie Loisel, Glen M. MacDonald.

Formal analysis: Julie Loisel, Marcus J. Thomson.

Funding acquisition: Glen M. MacDonald.

Investigation: Julie Loisel.

Methodology: Julie Loisel.

Project administration: Glen M. MacDonald.

Supervision: Glen M. MacDonald.

Visualization: Julie Loisel.

Writing – original draft: Julie Loisel.

Writing – review & editing: Julie Loisel, Glen M. MacDonald, Marcus J. Thomson.

References

1. Garfin GA, Merideth JR, Black M, LeRoy S (Eds.) (2013) Assessment of climate change in the Southwest United States: a report prepared for the national climate assessment. Southwest Climate Alliance, Washington DC, Island Press.
2. Cook BI, Cook ER, Smerdon JE, Seager R, Williams AP, Coats S, Stahle DW, Villanueva Diaz J (2016) North American megadroughts in the Common Era: reconstructions and simulations. *WIREs Climate Change* <https://doi.org/10.1002/wcc.394>
3. Milly PCD, Betancourt J, Falkenmark M, Hirsch RH, Kundzewicz ZW, Lettenmaier DP, Stouffer RJ (2008) Stationarity is dead: whither water management? *Science* 319: 573–574. <https://doi.org/10.1126/science.1151915> PMID: 18239110
4. Reilly JM (2002) Agriculture: the potential consequences of climate variability and change for the United States. Cambridge University Press, New York.
5. Polade SD, Pierce DW, Cayan DR, Gershunov A, Dettinger MD (2014) The key role of dry days in changing regional climate and precipitation regimes. *Scientific reports* 4.
6. Challinor AJJ, Watson DB, Lobell SM, Howden DR, Smith, Chhetri N (2014) A meta-analysis of crop yield under climate change and adaptation. *Nature Climate Change* 4: 287–291.
7. Westerling AL, Swetnam TW (2003) Interannual to decadal drought and wildfire in the western United States. *Eos Transactions AGU* 84(49):554–555.
8. Brown PM, Wu R (2005) Climate and disturbance forcing of episodic tree recruitment in a southwestern ponderosa pine landscape. *Ecology* 86(11):3030–3038.
9. Zylstra ER, Steidl RJ, Swann DE, Ratzlaff K (2015) Hydrologic variability governs population dynamics of a vulnerable amphibian in an arid environment. *PLoS ONE* 10(6): e0125670. <https://doi.org/10.1371/journal.pone.0125670> PMID: 26030825

10. Swetnam TW, Betancourt JL (2008) Mesoscale disturbance and ecological response to decadal climatic variability in the American Southwest. *Journal of Climate* 11:3128–3147.
11. Swetnam TW, Betancourt JL (2010) Mesoscale disturbance and ecological response to decadal climatic variability in the American Southwest. *Tree rings and natural hazards: a state-of-the-art*, eds Stofel M. et al. (Advances in Global Change Research 41, Springer) pp 329–359.
12. Swetnam TW, Baisan CH (2003) Tree-ring reconstructions of fire and climate history in the Sierra Nevada and southwestern United States. *Fire and climatic change in temperate ecosystems of the Western Americas*, eds Veblen TT, Baker WL, Montenegro G, Swetnam TW (Ecological Studies 160, Springer-Verlag), pp158–195.
13. Taylor AH, Trouet V, Skinner CN (2008) Climatic influences on fire regimes in montane forests of the southern Cascades, California, USA. *International Journal of Wildland Fire* 17:60–71.
14. Dettinger MD, Ralph FM, Das T, Neiman PJ, Cayan DR (2011) Atmospheric rivers, floods, and the water resources of California. *Water* 3: 445–478.
15. Hamlet AF & Lettenmaier DP (2007) Effects of 20th century warming and climate variability on flood risk in the western US. *Water Resources Research* 43(6).
16. Cayan DR, Dettinger MD, Diaz HF, Graham NE (1998) Decadal variability of precipitation over Western North America. *Journal of Climate* 11:3148–3166.
17. Cayan DR, Dettinger MD, Pierce D, Das T, Knowles N, Ralph FM, Sumargo E (2016) Natural variability, anthropogenic climate change, and impacts on water availability and flood extremes in the Western United States. *Water Policy and Planning in a Variable and Changing Climate*, 17.
18. Seager R, et al. (2005a) Mechanisms of ENSO-forcing of hemispherically symmetric precipitation variability. *Q.J.R. Meteorol. Soc.* 131:1501–1527.
19. Seager R, Kushnir Y, Herweijer C, Naik N, Velez J (2005b) Modeling of tropical forcing of persistent droughts and pluvials over Western North America: 1856–2000. *Journal of Climate* 18:4065–4088.
20. Cai W, et al. (2014) Increasing frequency of extreme El Niño events due to greenhouse warming. *Nature Climate Change* 4:111–116.
21. Taschetto AS, et al. (2014) Cold tongue and warm pool ENSO events in CMIP5: mean state and future projections. *Journal of Climate* 27:2861–2885.
22. Lübbecke JF, McPhaden MJ (2014) Assessing the twenty-first-century shift in ENSO variability in terms of the Bjerknes stability index. *Journal of Climate*. <https://doi.org/10.1175/JCLI-D-13-00438.1>
23. McGregor S, Timmermann A, Timm O (2010) A unified proxy for ENSO and PDO variability since 1650. *Climate of the Past* 6:1–17.
24. Cook BI, Ault TR, Smerdon JE (2015) Unprecedented 21st century drought risk in the American Southwest and Central Plains. *Science Advances* <https://doi.org/10.1126/sciadv.1400082> PMID: 26601131
25. Seager R, et al. (2007) Blueprints for Medieval hydroclimate. *Quaternary Science Reviews* 26:2322–2336.
26. MacDonald GM, Stahle DW, Villanueva Diaz J, Beer N, Busby SJ, Cerano-Paredes J, Cole JE, et al. (2008) Climate warming and 21st-century drought in Southwestern North America. *EOS, Transactions American Geophysical Union* 89(9): 82–82.
27. Mann ME, et al. (2009) Global signatures and dynamical origins of the Little Ice Age and Medieval Climate Anomaly. *Science* 326:1256–1260. <https://doi.org/10.1126/science.1177303> PMID: 19965474
28. Graham NE, Ammann CM, Fleitmann K, Cobb KM, Luterbacher J (2011) Support for global climate reorganization during the “Medieval Climate Anomaly”. *Climate Dynamics* 37:1217–1245.
29. Trouet V, et al. (2009) Persistent positive North Atlantic Oscillation mode dominated the Medieval Climate Anomaly. *Science* 324:78–80. <https://doi.org/10.1126/science.1166349> PMID: 19342585
30. Bradley RS, Wanner H, Diaz HF (2016) The Medieval Quiet Period. *The Holocene* 1–4, <https://doi.org/10.1177/0959683615622552>
31. Woodhouse CA, Overpeck JT (1998) 2000 years of drought variability in the Central United States. *Bulletin of the American Meteorological Society* 79(12):2693–2714.
32. Cook ER, Meko DM, Stahle DW, Cleaveland MK (1999) Drought reconstructions for the continental United States. *Journal of Climate* 12:1145–1162.
33. Meko DM, Therrell MD, Baisan CH, Hughes MK (2001) Sacramento River flow reconstructed to AD 869 from tree rings. *Journal of the American Water Resources Association* 37(4):1029–1039.
34. Herweijer C, Seager R, Cook ER (2006) North American droughts of the mid to late nineteenth century: a history, simulation and implication for Mediaeval drought. *The Holocene* 16(2):159–171.
35. Herweijer C, Seager R, Cook ER, Emile-Geay J (2007) North American droughts of the last millennium from a gridded network of tree-ring data. *Journal of Climate* 20:1353–1376.

36. Woodhouse CA, Russell JL, Cook ER (2009) Two modes of North American drought from instrumental and paleoclimatic data. *Journal of Climate* 22:4336–4347.
37. Woodhouse CA, Meko DM, MacDonald GM, Stahle DW, Cook ER (2010) a 1,200-year perspective of 21st century drought in southwestern North America. *Proceedings of the National Academy of Sciences of the USA* 107(50): 21283–21288. <https://doi.org/10.1073/pnas.0911197107> PMID: 21149683
38. Li J, et al. (2011) Interdecadal modulation of El Niño amplitude during the past millennium. *Nature Climate Change* 1:114–118.
39. Cook ER, Woodhouse CA, Eakin CM, Meko DM, Stahle DW (2004) Long-term aridity changes in the western United States. *Science* 306:1015–1018. <https://doi.org/10.1126/science.1102586> PMID: 15472040
40. Cook ER, et al. (2008) North American Summer PDSI Reconstructions, Version 2a. IGBP PAGES/World Data Center for Paleoclimatology Data Contribution Series # 2008–046. NOAA/NGDC Paleoclimatology Program, Boulder CO, USA.
41. Conroy JL, Overpeck JT, Cole JE, Steinitz-Kannan M (2009) Variable oceanic influences on western North American drought over the last 1200 years. *Geophysical Research Letters* 36:L17703.
42. Cobb KM, Charles CD, Cheng H, Edwards RL (2003) El Niño/Southern Oscillation and tropical Pacific climate during the last millennium. *Nature* 424:271–276. <https://doi.org/10.1038/nature01779> PMID: 12867972
43. Otto-Bliesner BE, Brady EC, Fasullo J, Jahn A, Landrum L, Stevenson S, Rosenbloom N, Mai A, Strand G (2016) Climate variability and change since 850 C.E.: an ensemble approach with the Community Earth System Model (CESM). *BAMS*, 735–754. <https://doi.org/10.1175/BAMS-D-14-00233.1>
44. Paillard D, Labeyrie L, Yiou P (1996) Macintosh program performs time-series analysis. *Eos Transactions AGU* 77:379.
45. D'Arrigo R, Cook ER, Wilson RJ, Allan R, Mann ME (2005) On the variability of ENSO over the past six centuries. *Geophysical Research Letters* 32, L03711.
46. Torrence C, Compo GP (1998) A practical guide to wavelet analysis. *Bulletin of the American Meteorological Society* 79(1): 61–78.
47. Gouhier T (2014) Biwavelet: conduct univariate and bivariate wavelet analyses (version 0.17.4). Available from <http://github.com/tgouhier/biwavelet>.
48. Lean J, Beer J, Bradley R (1995) Reconstruction of solar irradiance since 1610: implications for climate change. *Geophysical Research Letters* 22(23):3195–3198.
49. Crowley TJ (2000) Causes of climate change over the past 1000 years. *Science* 289:270–277. PMID: 10894770
50. Bard E, Raisbeck GM, Yiou F, Jouzel J (1997) Solar modulation of cosmogenic nuclide production over the last millennium: comparison between ¹⁴C and ¹⁰Be records. *Earth and Planetary Science Letters* 150(3–4):453–462.
51. Crowley TJ, Unterman MB (2013) Technical details concerning development of a 1200 yr proxy index for global volcanism. *Earth system Science Data* 5:187–197.
52. Moberg A, Sonechkin DM, Holmgren K, Datsenko NM, Wibjörn K (2005) Highly variable Northern Hemisphere temperatures reconstructed from low- and high-resolution proxy data. *Nature* 433:613–617. <https://doi.org/10.1038/nature03265> PMID: 15703742
53. Goosse H, Renssen H, Timmermann A, Bradley RS, Mann ME (2006) Using paleoclimate proxy-data to select optimal realisations in an ensemble of simulations of the climate of the past millennium. *Climate Dynamics* 27:165–184.
54. Coats S, Smerdon JE, Seager R, Cook BI, Gonzalez-Rouco JF (2013) Megadroughts in Southwestern North America in ECHO-G millennial simulations and their comparison to proxy drought reconstructions. *Journal of Climate* 26: 7635–7649.
55. Adams JB, Mann ME, Ammann CM (2003) Proxy evidence for an El Niño-like response to volcanic forcing. *Nature* 426:274–278. <https://doi.org/10.1038/nature02101> PMID: 14628048
56. Crowley TJ, et al. (2008) Volcanism and the Little Ice Age. *PAGES News* 16(2):22–23.
57. McGregor S, Timmermann A (2011) The effect of explosive tropical volcanism on ENSO. *Journal of Climate* 24: 2178–2191. <https://doi.org/10.1175/2010JCLI3990.1> 2011
58. Taylor KE, Stouffer RJ, Meehl GA (2012) A summary of the CMIP5 experiment design. *Bull Am Meteorol Soc* 93:485–498.
59. Myhre G et al. (2013) Anthropogenic and natural radiative forcing. In: Climate Change 2013: The physical science basis. Contribution of Working Group I to the Fifth Assessment Report of the Intergovernmental Panel on Climate Change, Stocker TF et al. (Eds.). Cambridge University Press, United Kingdom and New York, NY, USA.

60. McGregor HV, et al. (2015) Robust global ocean cooling trend for the pre-industrial Common Era. *Nature Geoscience* 8: 671–678. <https://doi.org/10.1038/ngeo2510>
61. Karnauskas BK, Smerdon JE, Seager R and Gonzalez-Rouco JF (2012) A Pacific centennial oscillation predicted by coupled GCMs. *Journal of Climate* 25: 5943–5961.
62. Smerdon JE, Coats S, Ault TR (2015) Model-dependent spatial skill in pseudoproxy experiments testing climate field reconstruction methods for the Common Era. *Climate Dynamics* 2684, <https://doi.org/10.1007/s00382-015-2684-0>
63. Cane MA (2005) The evolution of El Nino, past and future. *Earth and Planetary Science Letters* 230: 227–240.
64. MacDonald GM, et al. (2016) Prolonged California aridity linked to climate warming and Pacific sea surface temperature. *Scientific Reports* <https://doi.org/10.1038/srep33325> PMID: 27629520
65. Cai W, et al. (2012) More extreme swings of the South Pacific convergence zone due to greenhouse warming. *Nature* 488: 365–370. <https://doi.org/10.1038/nature11358> PMID: 22895343
66. Yeh S-W, Kirtman BP (2007) ENSO amplitude changes due to climate change projections in different coupled models. *Journal of Climate* 20:203–217.
67. Collins M, et al. (2010) The impact of global warming on the tropical Pacific Ocean and El Niño. *Nature Geoscience* 3:391–397.
68. Timmerman A (1999) Detecting the nonstationary response of ENSO to greenhouse warming. *Journal of Climate* 56:2313–2325.
69. Newton A, Thunell R, Stott L (2006) Climate and hydrographic variability in the Indo-Pacific Warm Pool during the last millennium. *Geophysical Research Letters* 33, L19710, <https://doi.org/10.1029/2006GL027234>
70. Brown JN, Langlais C, Maes C (2014) Zonal structure and variability of the Western Pacific dynamic warm pool edge in CMIP5. *Climate Dynamics* 42:3061–3076.
71. Brown JN, Langlais C, Gupta AS (2015) Projected sea surface temperature changes in the equatorial Pacific relative to the Warm Pool edge. *Deep-Sea Research II* 113:47–58.
72. Lewis SC, LeGrande AN (2015) Stability of ENSO and its tropical Pacific teleconnections over the Last Millennium. *Climate of the Past* 11: 1347–1360.
73. Meko DM, et al. (2007) Medieval drought in the upper Colorado River basin. *Geophysical Research Letters* 34, <https://doi.org/10.1029/2007GL029988>
74. MacDonald GM (2007) Severe and sustained drought in southern California and the West: Present conditions and insights from the past on cause and impacts. *Quaternary International* 173–174:87–100.
75. MacDonald GM (2010) Water, climate change, and sustainability in the southwest. *Proceedings of the National Academy of Sciences of the USA* 107(50): 21256–21262. <https://doi.org/10.1073/pnas.0909651107> PMID: 21149704
76. Wang S-Y, Davies RE, Gillies RR (2013), Identification of extreme precipitation threat across mid-latitude regions based on shortwave circulations, *Journal of Geophysical Research—Atmosphere*, 118: 11,059–11,074. <https://doi.org/10.1002/jgrd.50841>
77. Wang S-Y, Hipps L, Gillies RR, Yoon J-H (2014) Probable causes of the abnormal ridge accompanying the 2013–2014 California drought: ENSO precursor and anthropogenic warming footprint. *Geophysical Research Letters* 41: 3220–3226, <https://doi.org/10.1002/2014GL059748>
78. Raje D, Mujumdar PP (2010) Reservoir performance under uncertainty in hydrologic impacts of climate change. *Advances in Water Resources* 33(3): 312–326.
79. Dettinger M (2011) Climate change, atmospheric rivers, and floods in California—a multimodel analysis of storm frequency and magnitude changes. 47(3): 514–523.
80. Power MJ, et al. (2008) Changes in fire regimes since the Last Glacial Maximum: an assessment based on a global synthesis and analysis of charcoal data. *Climate Dynamics* 30: 887–907.
81. Power MJ, et al. (2012) Climatic control of the biomass-burning decline in the Americas after AD 1500. *The Holocene* <https://doi.org/10.1177/0959683612450196>
82. Daniau A-L, et al. (2012) Predictability of biomass burning in response to climate changes. *Global Biogeochemical Cycles* 26:GB4007, <https://doi.org/10.1029/2011GB004249>
83. Marlon JR, et al. (2012) Long-term perspective on wildfires in the western USA. *Proceedings of the National Academy of Sciences of the USA* <https://doi.org/10.1073/pnas.1112839109> PMID: 22334650
84. Marlon JR, et al. (2013) Global biomass burning: a synthesis and review of Holocene paleofire records and their controls. *Quaternary Science Reviews* 65:5–25.
85. Westerling AL, Hidalgo HG, Cayan DR, Swetnam TW (2006) Warming and earlier spring increase western US forest wildfire activity. *Nature* 313:940–943.

86. Polade SD, Gershunov A, Cayan DR, Dettinger MD, Pierce DW (2017) Precipitation in a warming world: Assessing projected hydro-climate changes in California and other Mediterranean climate regions. *Scientific Reports* 7: 10783, <https://doi.org/10.1038/s41598-017-11285-y> PMID: 28883636